Article

Not peer-reviewed version

A Customized 3D Printed Bolus for High-Risk Breast Cancer with Skin Infiltration: A Pilot Study

Silvia Takanen *, Anna Ianiro *, Paola Pinnaro, Erminia Infusino *, Laura Marucci, Antonella Soriani, Giuseppe Sanguineti, Giuseppe Iaccarino

Posted Date: 16 August 2024

doi: 10.20944/preprints202408.1253.v1

Keywords: breast cancer; skin toxicity; dosimetric analysis; 3D printed bolus

 doi:10.20944/preprints202408.1253.v1

Article

A Customized 3D Printed Bolus for High-Risk Breast Cancer with Skin Infiltration: A Pilot Study

Silvia Takanen [1,*], Anna Ianiro [2], Paola Pinnaro [1], Erminia Infusino [2,*], Laura Marucci [1], Antonella Soriani [2], Giuseppe Sanguineti [1] and Giuseppe Iaccarino [2]

[1] Radiation Oncology Department, IRCCS Regina Elena National Cancer Institute, Rome, Italy
[2] Medical Physics Department, IRCCS Regina Elena National Cancer Institute, Rome, Italy
* Correspondence: silvia.takanen@ifo.it (S.T.); erminia.infusino@ifo.it (E.I.)

Simple Summary: In high-risk breast cancer patients with skin infiltration the use of a bolus positioned at the patient's skin is required to guarantee therapeutic dose delivery to superficial tissues, in order to reduce local skin relapse. A personalized bolus may prevent the potential standard bolus' inadequate dose distribution due to air gaps between the bolus and the skin, improving target coverage. In this pilot study, we introduced in clinical practice the use of a personalized 3D printed bolus filled with ultrasound transmission gel, which should permit to reproduce the standard bolus' consistency, providing an adequate coverage of the target area.

Abstract: Background: In high-risk breast cancer patients with skin infiltration the administration of a uniform dose to superficial tissues is fundamental in order to reduce local skin relapse. A personalized bolus may prevent the potential standard bolus' inadequate dose distribution due to air gaps between the bolus and the skin. In this pilot study, we introduced in clinical practice the use of a personalized 3D printed bolus filled with ultrasound transmission gel. Methods: Seven patients undergoing radiotherapy after mastectomy were selected. 3D printed bolus dosimetric assessment was performed with MOSFET dosimeters on an anthropomorphic phantom and subsequently on three selected cases with increasing bolus shape irregularity. Acute/late toxicity and local control was assessed. Results: Overall, for the clinical cases the percentage median difference between measured and calculated doses was -2.7% (-7.0%÷4.9%). Median follow-up was 21 months. After two years, one patient showed G2 pain, one patient manifested G1 telangiectasia, one patient showed G1 hyperpigmentation, and two patients had no relevant toxicity. Conclusions: Personalized 3D-printed bolus filled with ultrasound gel may easily reproduce the standard bolus' consistency providing an accurate coverage of the target area with tolerable acute/late toxicity grades. This is a pilot study and further investigations are needed.

Keywords: breast cancer; skin toxicity; dosimetric analysis; 3D printed bolus

1. Introduction

In high-risk breast cancer (BC) patients undergoing mastectomy, radiation therapy (RT) plays a fundamental role reducing the risk of loco-regional relapse (LRR) and improving overall survival (OS) [1]. The use of a slab of solid water-like material, named bolus, positioned at the patient's skin is required to guarantee therapeutic dose delivery to superficial tissues, including the skin. The use of bolus for all breast cancer patients after post-mastectomy radiotherapy (PMRT) is still debated due to skin toxicity, as evidenced in a variety of studies, clinician surveys, and international guidelines [2]. All studies showed differences in bolus utilization, scheduling (i.e., daily, alternating days), material, and RT planning characteristics. Due to the lack of randomized trials evaluating the benefits of bolus, a recent international consensus discussed current evidence about the use of bolus in the setting of PMRT and its effect on LRR and toxicity [3].

 doi:10.20944/preprints202408.1253.v1

In our center, we prescribe the use of bolus in patients with skin infiltration and epidermal-dermal involvement (T4b), to cover the area of the skin and subcutaneous tissues at high risk of relapse with at least 95% of the prescribed dose [2].

Achieving the optimal fit of the bolus on the chest wall, particularly in case of immediate reconstruction with prosthesis is difficult. In recent years, the realization of 3D personalized bolus printing for RT has shown an increasing interest [4–6]. In this pilot study, we selected BC patients with skin involvement, with or without immediate reconstruction, introducing a new 3D printed bolus filled with ultrasound transmission gel to reproduce the standard bolus' consistency and provide an adequate coverage of the target area. Its use was primarily validated on an anthropomorphic phantom with MOSFET in-vivo dosimetry and then was applied in clinical practice.

2. Materials and Methods

2.1. Patients

Seven patients with high risk BC and pathological skin involvement, following mastectomy with or without immediate reconstruction, underwent chest wall RT from January to November 2021. The median age was 64.5 years (range: 45÷82 years).

Four patients had chest wall skin relapse after a prior mastectomy. Two patients had a postoperative pathological exam revealing skin infiltration; one patient was staged cT4b before neoadjuvant systemic therapy and ypT4b after surgery. Three patients underwent immediate breast reconstruction with prosthesis.

RT was delivered at the target site (chest wall with or without loco-regional lymph nodes) in 25 daily fractions with a total dose of 50 Gy.

Each patient was clinically evaluated at 1 week, at 3 months, at 6 months, at 1 year and at 2 years from the end of RT. Acute/late toxicity and local control (LC) were assessed for each patient.

2.3. Bolus manufacture procedure

The procedure adopted to introduce the use of a personalized bolus in clinical practice is composed of the following steps, starting from computed tomography (CT) acquisition up to bolus printing.

CT images were acquired with a Philips Big Bore scanner (Koninklijke Philips N.V., Netherlands), with a slice thickness of 1.5 mm. Patient setup involved the use of a wing board with the patient in supine position and arms up. Before CT scan acquisition, four radiopaque markers were placed on the patient's surface as reference points to longitudinally and laterally delimit the region for bolus location (bolus setup markers). In addition, three markers were placed at the same axial plane for patient setup: one at sternum location and two at patient sides (patient setup markers).

CT images of the patient were imported into Eclipse (Varian Medical Systems Inc., USA) treatment planning system (TPS), version 15.6. The body, the planning target volume (PTV) comprising the breast with or without loco-regional lymph nodes, and the main organs at risk (OARs) were contoured. The PTV was delineated including the whole breast up to the skin.

A bolus with a thickness of 7 mm was delineated on the patient CT, using the Eclipse TPS bolus tool. A primary automated shape of the bolus, created inside a virtual box, was confined to a maximum distance of 2 cm from PTV extremities.

The virtual bolus structure was further modified to guide its correct positioning on the patient. Cuts were created at the position of the bolus setup markers, as shown in Figure 1.

 doi:10.20944/preprints202408.1253.v1

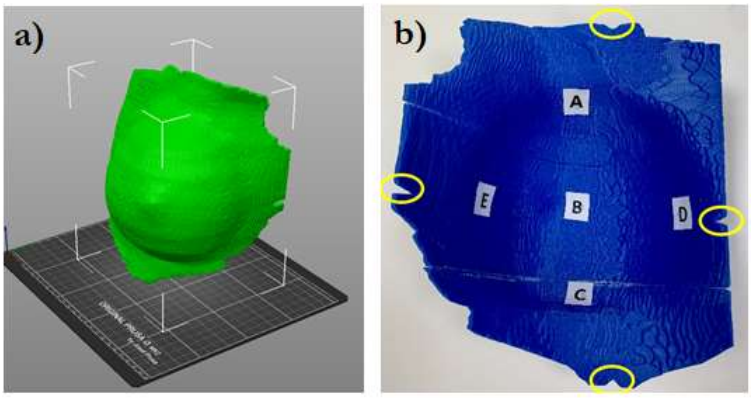

Figure 1. 3D Bolus rendering (a) and inner side of the bolus (b). Letters A (cranial), B (central), C (caudal), D (medial), E (external) represent MOSFET dosimeters positioning. The circles indicate the position of the cuts for bolus alignment.

Five small spherical ROIs were contoured at positions where the skin point dose will be evaluated. The five ROIs were subtracted from the inner surface of the bolus ROI and used to create a suitable housing for MOSFET dosimeters positioning (Figure 2). Thus, for the following dosimetric evaluation the position of the MOSFETs inside the printed bolus corresponded to the ROIs contoured on the TPS.

The bolus structure in DICOM format was imported into 3DSlicer [7], an open-source software that enables the conversion of the DICOM file into standard tessellation language (STL) format. The STL file was then imported into the PrusaSlicer-2.3.3 software [8] of the Prusa i3 MK2S printer and converted into the gcode printer format.

The bolus is manufactured in polylactic acid (PLA), a fully biodegradable and nontoxic plastic with an electron density relative to water of 1.1-1.2, approximately [5]. The printing resolution (layer height) was set to 0.2 mm. The extruder and bed temperature of the 3D printer were maintained at 215 °C and 60 °C, respectively.

Boluses exceeding the maximum printing volume allowed (25×21×20 cm3), were printed in two or three separate pieces that were joined together using glue. Each part was printed as an empty rigid container with walls having a thickness of 1.5 mm and then filled with ultrasound transmission gel (Gel G006 ECO, Fiab, Italy), having a density similar to water (20-30 HU). This technique ensured that the characteristics of attenuation and weight of the 3D printed bolus were similar to a traditional gel bolus. A CT scan of the 3D bolus was acquired to check for the presence of accidental air bubbles.

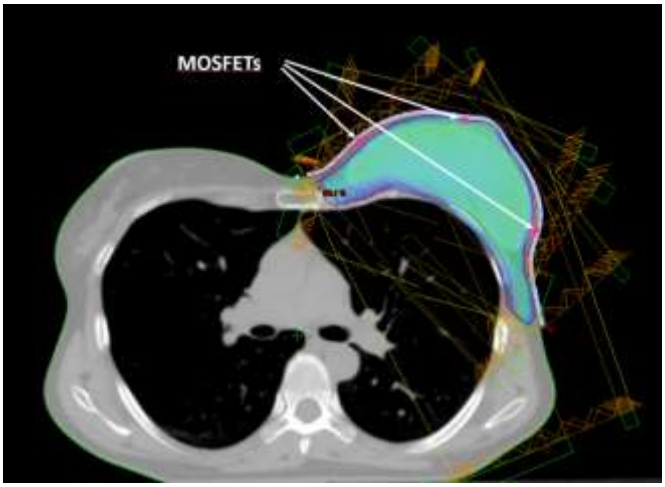

Figure 2. Beam arrangement for IMRT dose delivery. Isodose of 95% of prescribed dose. Positions of the three middle height MOSFETs.

 doi:10.20944/preprints202408.1253.v1

2.4. Treatment planning

The treatment technique employed for both the phantom and patients involved four to six intensity modulated (IMRT) tangential beams, with half using medial and half using external entries, in sliding window delivery mode. All beams had a dose rate of 600 MU/min and a photon energy of 6 MV produced by a TrueBeam linear accelerator (Varian Medical Systems Inc., USA).

Treatment plans were optimized using the Eclipse TPS inverse planning photon optimizer module. Dose objectives for target and OARs were set to meet the internal protocol tolerances. Dose calculation was performed with the Eclipse analytical anisotropic algorithm (AAA), which is a convolution-superposition-based photon dose computation algorithm [9]. A calculation grid size of 2.5 mm was used. After dose calculation, plans were normalized to ensure 100% of the prescribed dose to the PTV mean dose (Dmean).

The mean doses calculated in the five ROIs representing dosimeter locations were recorded and compared with measurements.

A cone beam CT (CBCT) was acquired before each treatment delivery, to verify the correct patient positioning and bolus fitting.

2.5. In-vivo dosimetry equipment

In-vivo dosimetry was performed with MOSFET dosimeters (Best Medical International, Canada). The choice was based on certain characteristics that make MOSFETs suitable sensors for in-vivo dosimetry, such as low energy dependence, high sensitivity, and direct reading capabilities.

Specifically, both the standard model (TN-502RD-H) and the microMOSFET model (TN-502RDM-H) were used. These dosimeters operated in conjunction with the Patient Dose Verification System (model TN-RD-16), with the high sensitivity bias supply setting. A TN-RD-38 Bluetooth transceiver was used for real-time data communication between the TN-RD-16 reader and a PC where the MOSFET software was installed. The software can assign calibration factors, correction factors, and target dose to each dosimeter.

The size of the standard MOSFET and the size of the microMOSFETs are 8.0×2.5×1.3mm3 and 3.5×1.0×1.3mm3, respectively. The active area is 2×10-5 mm3 [10].

The dose delivered (cGy) is proportional to the difference in voltage shift before and after exposure (mV).

A calibration factor (cGy/mV) was determined for each MOSFET following standard procedures.

Before beam delivery, five background readings were acquired and their average was used to correct the subsequent measurements.

2.6. Phantom dosimetry

A dosimetric investigation of the 3D printed bolus was primarily conducted on an anthropomorphic phantom, Rando® (The Phantom Laboratory, Salem, NY). This phantom is radiologically equivalent to an actual human body and comprises a special thermosetting synthetic rubber molded around a natural human skeleton. The phantom is equipped with two breasts composed of the same tissue-equivalent rubber, which can be secured on its surface with plastic screws [11,12].

A treatment plan was calculated on phantom CT as described in the treatment planning section. The plan was delivered five times with the dosimeters placed at the same positions to assess delivery reproducibility.

2.7. Patient dosimetry

MOSFET in vivo-dosimetry was performed on three selected clinical cases, each exhibiting increasing bolus shape irregularity. The first case involved patients with chest wall skin relapse after a prior mastectomy with an almost flat and regular bolus shape. The second case involved patients with chest wall skin relapse after a prior mastectomy and nodal involvement, where raised post-

 doi:10.20944/preprints202408.1253.v1

surgery scars requires the printing of an irregular-shaped bolus. The third case involved patients with prosthesis after mastectomy for local relapse for whom a bolus with a particularly convex shape is needed.

For each patient, in-vivo dosimetry was performed once a week, totaling five sessions.

3. Results

3.1. Dosimetric results

MOSFET calibration factors ranged between 0.90÷0.93 cGy/mV, with an average of 0.91±0.01 cGy/mV.

Figure 3 shows the percentage difference between measured and calculated doses for the phantom and the selected clinical cases.

Overall, for the clinical cases the percentage difference ranged from -7.0% to +4.9%, with a median value of -2.7%. Moreover, the median absolute dose measured with dosimeters was 47.7 Gy [44.0÷50.8 Gy].

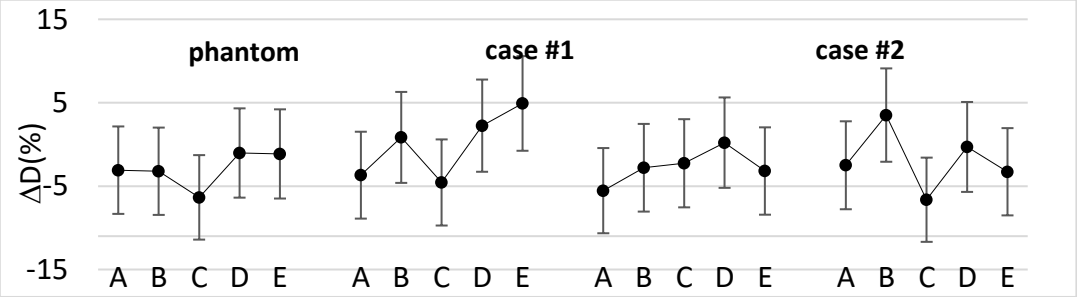

Figure 3. Percentage difference between measured and calculated doses for the phantom and three clinical cases with increasing bolus shape irregularity at the five MOSFET positions.

3.2. Clinical results

The median follow-up (fup) was 21 months (1÷26 months).

Acute and late toxicity were assessed according to Common terminology criteria for adverse effects (CTCAE) v.5.0 scale [13] and LENT SOMA scale [14], respectively.

At 1 week from the treatment, grade 1 (G1) and grade 2 (G2) skin toxicity were observed in 3 and 4 patients, respectively.

After three months, 3 patients showed G1 hyperpigmentation. One patient had no relevant toxicity. One of the patients with immediate reconstruction after mastectomy for LRR complained G1 local pain associated with skin desquamation around the prosthesis. One patient had nodular skin relapse and died for local and distant disease progression. One patient was lost to fup.

At six months and at one year there was no significant variation, except for the patient with prosthesis that complained a worse G2 local pain.

After one year, G2 local pain persisted in the patient with prosthesis. One patient had G1 telangiectasia, one patient showed G1 hyperpigmentation and 2 patients had no relevant toxicity.

At two years, the patient with prosthesis required surgical intervention to replace the prosthesis. No significant change was recorded for the remaining patients.

Figure 4 resumes the results observed for the main endpoints analysed at follow-up (erythema, pain, hyperpigmentation, and telangiectasia).

 doi:10.20944/preprints202408.1253.v1

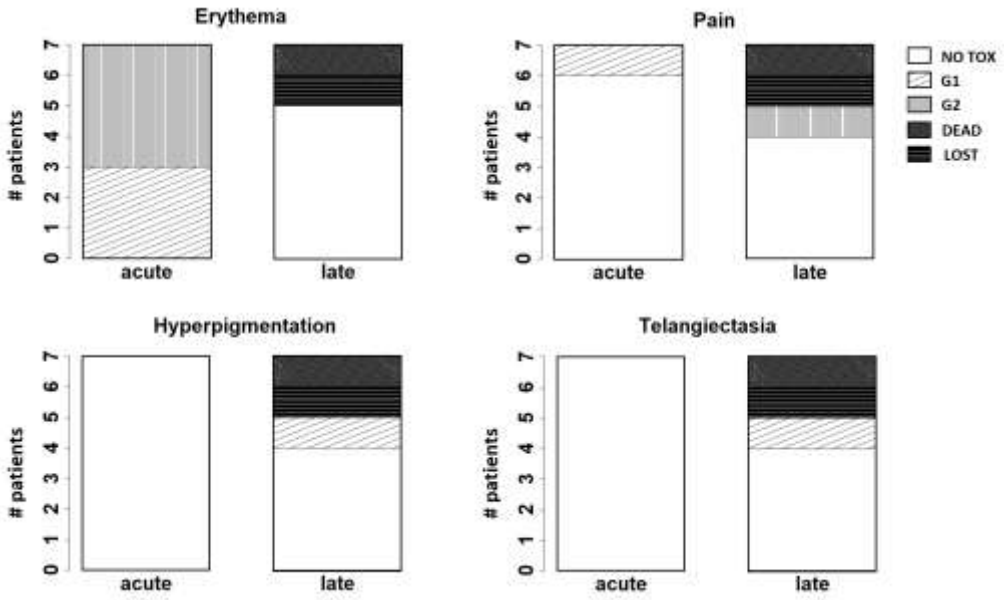

Figure 4. Bar plots for the main endpoints analysed at follow-up (erythema, pain, hyperpigmentation, and telangiectasia). "Acute" refers to the results observed at the first week after treatment; "late" refers to the results observed at two years after treatment.

4. Discussion

In this study, the use of a 3D printed bolus composed of a personalized shape container in PLA filled with an ultrasound gel emulsion with physical characteristic similar to water, was introduced in the clinical practice in the context of a pilot study for patients undergoing mastectomy with or without immediate breast reconstruction.

After preclinical studies, 3D-printed boluses seemed to overcome the disadvantages of traditionally available boluses reducing air gaps in order to achieve doses closer to a uniform prescription.

Some studies [15–20] have analyzed the characteristics of different materials for 3D personalized bolus printing and are based on preliminary investigations on phantoms. Only few studies demonstrated the efficacy of applying 3D printed boluses to actual patients in BC. Robar et al. [5] compared the use of a 3D printed bolus with the use of a standard SuperFlab sheet bolus for 16 patients who underwent chest wall PMRT, demonstrating a better fitting of the 3D printed bolus to the skin. Canters et al. [4] used a 3D shell as a mold to create a silicone bolus for the treatment of 11 non-melanoma skin cancer patients, showing that the 3D printing process was efficient and that the custom bolus satisfied the required dosimetric objectives.

In this study, the use of the 3D bolus filled with an ultrasound gel emulsion was primarily validated on a phantom assessing that the dose measured at phantom surface with MOSFET dosimeters was in agreement with the dose calculated by the TPS. Subsequently, it was applied to patients by checking their surface dose. Figure 3 shows that in most cases the difference between measured and calculated doses was within dosimeters reproducibility range (± 4.5%) [21] combined with AAA dose calculation uncertainty at 7mm depth (± 3%) [22]. The outliers can be explained considering that the dose was delivered with tangential fields and referred to points where phantom or patient surface was steeper. However, the magnitude of the differences is in the range of the results found in previous works [5,23].

Ensuring adequate contact with the skin using a standard bolus is challenging. Air gaps between bolus and skin can lead to an inadequate or inhomogeneous radiation dose delivery to the surface of the skin. At the medial and lateral borders, where the beam axis is more perpendicular to the skin, a relative dose coverage deficit near the skin is critical (Figure 5).

 doi:10.20944/preprints202408.1253.v1

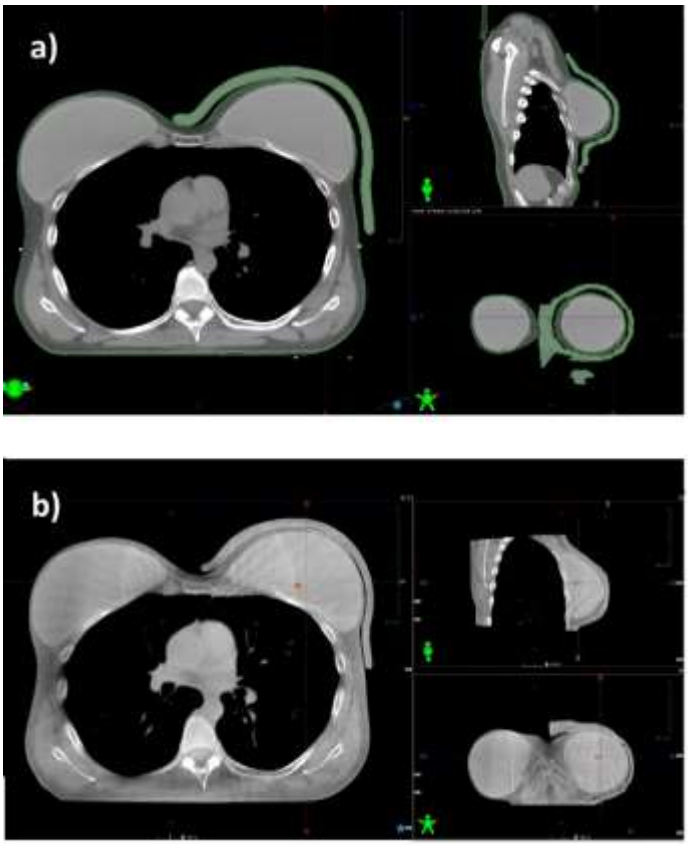

Figure 5. CT scan of a patient with prosthesis and standard gel bolus (a) and CBCT acquired before radiation delivery in the same patient (b). 3D bolus fits the skin without relevant air gaps.

On the basis of daily CBCT acquisition, we observed that the positioning of the 3D bolus is reproducible and its shape better conforms to the skin, visibly reducing air gaps. Quantitative air gap analysis was previously described in literature [5,20]. The personalized shape of the 3D-bolus makes it similar to a custom immobilization device, simplifying patient positioning, reducing setup time, and improving patient compliance. This represents a significant advantage for the patient. However, the whole printing process can be time-consuming and cumbersome to manage for the operator.

Regarding the main outcomes, such as toxicity and LC, there is still a significant lack of data in literature supporting the use of bolus for PMRT, with or without immediate reconstruction. A recent review [24] showed that the use of bolus with PMRT was associated with similar LRR rates (3.5% with bolus vs. 3.6% without) but increased acute toxicity (9.6% with bolus vs. 1.2% without), when compared to PMRT without bolus. The authors suggest that in case of skin involvement (T4b-d) or multiple high-risk features for LRR, including positive margins, extensive lympho-vascular invasion and triple-negative subtype, the use of bolus could be recommended to achieve an adequate dose to the superficial chest wall structures (skin and subcutaneous tissue). Nichol et al. [6] observed that, after mastectomy, the use of bolus doubles the risk of G2 and G3 skin toxicity and, on multivariable analysis, its use was not associated with better LC. Anderson et al. [23] analyzed the complications and cosmetic results related to the use of a custom wax bolus fitting the skin, showing that a customized bolus can significantly reduce the incidence of complications compared to traditional bolus sheets (9% vs 24%).

Both the traditional bolus and 3D-printed bolus not only increase the irradiation dose on the skin surface, but also aggravate the skin reaction to varying degrees. However, interpretation of the available pooled toxicity data in literature is limited by the variation in toxicity scales used across studies. In particular, little is known about the use of bolus in the hypofractionation setting and immediate breast reconstruction [25] and the different types of breast reconstruction (e.g., autologous vs. implant) for LRR, toxicity and reconstruction-related complications [24].

 doi:10.20944/preprints202408.1253.v1

In our pilot investigation, we reported G2 radiation dermatitis as the maximum and more frequent acute side effect. At two years' follow-up, the maximum late toxicity was G2 pain in one patient with prosthesis, G1 telangiectasia in one patient and G1 hyperpigmentation in another patient. Further investigations with a higher number of patients are needed. Moreover, to evaluate the efficacy in terms of LC of the 3D printed bolus filled with an ultrasound gel a longer fup is required.

5. Conclusions

The development of customized 3D-printed boluses has shown to reduce the air gap, improving the accuracy and uniformity of dose, better protecting normal tissues. However, there is a lack of scientific evidence regarding the use of 3D bolus and there is not yet a consensus about the material choice, and frequency of application. Our pilot study showed that a personalized 3D-printed filled with ultrasound gel may easily reproduce the standard bolus' consistency and provide an accurate coverage of the target area, especially in post-mastectomy radiotherapy with prosthesis, with tolerable acute/late toxicity grades. Further investigations with a higher number of patients and a longer fup are needed.

Author Contributions: S.T., P.P. and G.I. designed the study. S.T. and P.P. selected the patients and carried out clinical analysis. G.I. worked out almost all of the technical details, and performed the dosimetric measurements and data analysis with the support from A.I. and E.I. S.T. and A.I. equally contributed to manuscript writing with the supervision from G.I. L.M. revised the manuscript critically for important intellectual content. A.S. and G.S. supervised the findings of this work. All authors discussed the results and contributed to the final manuscript.

Funding: This work was financially supported through funding from the institutional "Ricerca Corrente" granted by the Italian Ministry of Health.

Institutional Review Board Statement: The pi was conducted in accordance with the Declaration of Helsinki and approved by COMITATO ETICO CENTRALE I.R.C.C.S. LAZIO Sezione IRCCS I.F.O. – Fondazione G.B. Bietti, Approval N° 0004393.25-03-2024.

Informed Consent Statement: Informed consent was obtained from all subjects involved in the study.

Conflicts of Interest: The authors declared no potential conflicts of interests associated with this study.

References

1. Recht, A.; Comen, E.A.; Fine, R.E.; Fleming, G.F.; Hardenbergh, P.H.; Ho, A.Y.; Hudis, C.A.; Hwang, E.S.; Kirshner, J.J.; Morrow, M.; Salerno, K.E.; Sledge, G.W. Jr; Solin, L.J.; Spears, P.A.; Whelan, T.J.; Somerfield, M.R.; Edge, S.B. Postmastectomy Radiotherapy: An American Society of Clinical Oncology, American Society for Radiation Oncology, and Society of Surgical Oncology Focused Guideline Update. *Pract. Radiat. Oncol.* **2016** *6*(6):e219-e234. 10.1016/j.prro.2016.08.009.
2. Kaidar-Person, O.; Dahn, H.M.; Nichol, A.M.; Boersma, L.J.; de Ruysscher, D.; Meattini, I.; Pignol, J.P.; Aristei, C.; Belkacemi, Y.; Benjamin, D.; Bese, N.; Coles, C.E.; Franco, P.; Ho, A.Y.; Hol, S.; Jagsi, R.; Kirby, A.M.; Marrazzo, L.;, Marta, G.N.; Moran, M.S.; Nissen, H.D.; Strnad, V.; Zissiadis, Y. A Delphi study and International Consensus Recommendations: The use of bolus in the setting of postmastectomy radiation therapy for early breast cancer. *Radiother. Oncol.* **2021** *164*:115-121. 10.1016/j.radonc.2021.09.012.
3. Dahn HM, Boersma LJ, de Ruysscher D, Meattini I, Offersen BV, Pignol JP, Aristei C, Belkacemi Y, Benjamin D, Bese N, Coles CE, Franco P, Ho A, Hol S, Jagsi R, Kirby AM, Marrazzo L, Marta GN, Moran MS, Nichol AM, Nissen HD, Strnad V, Zissiadis YE, Poortmans P, Kaidar-Person O. The use of bolus in postmastectomy radiation therapy for breast cancer: A systematic review. Crit. Rev. Oncol. Hematol. 2021 *163*:103391. 10.1016/j.critrevonc.2021.103391.
4. Canters, R.A.; Lips, I.M.; Wendling, M.; Kusters, M.; van Zeeland, M.; Gerritsen, R.M.; Poortmans, P.; Verhoef, CG. Clinical implementation of 3D printing in the construction of patient specific bolus for electron beam radiotherapy for non-melanoma skin cancer. *Radiother. Oncol*. **2016** *121*(1):148-153. 10.1016/j.radonc.2016.07.011.
5. Robar, J.L.; Moran, K.; Allan, J.; Clancey, J.; Joseph, T.; Chytyk-Praznik, K.; MacDonald, R.L.; Lincoln, J.; Sadeghi, P.; Rutledge, R. Intrapatient study comparing 3D printed bolus versus standard vinyl gel sheet

bolus for postmastectomy chest wall radiation therapy. *Pract Radiat Oncol.* **2018** *8*(4):221-229. 10.1016/j.prro.2017.12.008.

6. Nichol, A.; Narinesingh, D.; Raman, S.; Germain, F.; Chan, E.K.; Tran, E.; Gondara, L.; Speers, C.; Lohrisch, C.A.; Truong, P. The effect of bolus on local control for patients treated with mastectomy and radiation therapy. *Int. J. Radiat. Oncol. Biol. Phys.* **2021** *110*(5):1360-1369. 10.1016/j.ijrobp.2021.01.019.
7. 3D Slicer image computing platform. www.slicer.org. Accessed January **2021**.
8. PrusaSlicer-2.3.3 software. www.prusa3d.com. Accessed January **2021**.
9. Sievinen, J.; Ulmer, W.; Kaissl, W. AAA Photon Dose Calculation Model in Eclipse™. RAD #7170A.
10. Best Medical International, Canada. Technical Note 7: MOSFET Dosimeter Specifications | TN#101684.04.
11. Alderson, S.W.; Lanzl, L.H.; Rollins, M.; Spira, J. An instrumented phantom system for analog computation of treatment plans. *Am. J. Roentgenol. Radium. Ther. Nucl. Med.* **1962** *87*:185-95.
12. Saylor, W.L.; Adams, B.L. The patient equivalence of the RANDO phantom for cobalt gamma rays. *Radiology* **1969** *92*(1):165. 10.1148/92.1.165a.
13. Common Terminology Criteria for Adverse Events (CTCAE) Version 5.0, November 27, **2017**, National Cancer Institute (NCI).
14. LENT SOMA scales for all anatomic sites. Int. *J. Radiat. Oncol. Biol. Phys.* **1995** *31*(5):1049-91. 10.1016/0360-3016(95)90159-0.
15. Baltz, G.C.; Chi, P.M.; Wong, P.F.; Wang, C.; Craft, D.F.; Kry, S.F.; Lin, S.S.H.; Garden, A.S.; Smith, S.A.; Howell, R.M. Development and Validation of a 3D-Printed Bolus Cap for Total Scalp Irradiation. *J. Appl. Clin. Med. Phys.* **2019** *20*(3):89–96. doi: 10.1002/acm2.12552
16. Burleson, S.; Baker, J.; Hsia, A.T.; Xu, Z. Use of 3D printers to create a patient-specific 3D bolus for external beam therapy. *J. Appl. Clin. Med. Phys.* **2015** *16*(3):5247. 10.1120/jacmp.v16i3.5247.
17. Su, S.; Moran, K.; Robar, J.L. Design and production of 3D printed bolus for electron radiation therapy. *J. Appl. Clin. Med. Phys*. **2015** *15*(4):4831. 10.1120/jacmp.v15i4.4831.
18. Ju, S.G.; Kim, M.K.; Hong, C.S.; Kim, J.S.; Han, Y.; Choi, D.H.; Shin, D.; Lee, S.B. New technique for developing a proton range compensator with use of a 3-dimensional printer. Int. J. *Radiat. Oncol. Biol. Phys.* **2014** *88*(2):453-8. 10.1016/j.ijrobp.2013.10.024.
19. Khan, Y.; Villarreal-Barajas, J.; Udowicz, M.; Sinha, R.; Muhammad, W.; Abbasi, A. and Hussain, A. Clinical and Dosimetric Implications of Air Gaps between Bolus and Skin Surface during Radiation Therapy. *J. Cancer Ther.* **2013** *4*(7):1251-1255 10.4236/jct.2013.47147.
20. Butson, M.J.; Cheung, T.; Yu, P.; Metcalfe, P. Effects on skin dose from unwanted air gaps under bolus in photon beam radiotherapy. *Rad. Meas*. **2000** *32*(3):201-204. https://doi.org/10.1016/S1350-4487(99)00276-0.
21. Best Medical International, Canada. Technical Note 1: Dose Reproducibility Assessment | TN#101245.03.
22. Lundstedt, D.; Lindberg, A.; Gustafsson, M.; Chakarova, R.; Karlsson, P. Adjuvant Radiation Treatment of Breast Cancer After Mastectomy: Advanced Algorithms and Partial Bolus Improve the Dose Calculation Accuracy in the Case of Thin-Chest-Wall Irradiation. *Adv. Radiat. Oncol*. **2023** *8*(5):101223. 10.1016/j.adro.2023.101223.
23. Anderson, P.R.; Hanlon, A.L.; Fowble, B.L.; McNeeley, S.W.; Freedman, G.M. Low complication rates are achievable after postmastectomy breast reconstruction and radiation therapy. *Int. J. Radiat. Oncol. Biol. Phys*. **2004** *59*(4):1080-7. 10.1016/j.ijrobp.2003.12.036.
24. Jassem, J. Post-mastectomy radiation therapy after breast reconstruction: Indications, timing and results. *Breast* **2007** *34* Suppl 1:S95-S98. 10.1016/j.breast.2017.06.037.
25. Kim, D.Y.; Park, E.; Heo, C.Y.; Jin, U.S.; Kim, E.K.; Han, W.; Shin, K.H.; Kim, IA. Hypofractionated versus conventional fractionated radiotherapy for breast cancer in patients with reconstructed breast: Toxicity analysis. *Breast* **2021** *55*:37-44. 10.1016/j.breast.2020.11.020.